Phase structures and morphologies determined by competitions among self-organization, crystallization, and vitrification in a disordered poly(ethylene oxide)-*b*-polystyrene diblock copolymer

Lei Zhu, Yan Chen, Anqiu Zhang, Bret H. Calhoun, Moonseok Chun,
Roderic P. Quirk, and Stephen Z. D. Cheng*
Maurice Morton Institute and Department of Polymer Science, The University of Akron, Akron, Ohio 44325-3909

Benjamin S. Hsiao and Fengji Yeh
Department of Chemistry, The State University of New York at Stony Brook, Stony Brook, New York 11794-3400

Takeji Hashimoto
Department of Polymer Chemistry, Graduate School of Engineering, Kyoto University, Kyoto 606, Japan
(Received 11 February 1999)

A poly(ethylene oxide)-*b*-polystyrene (PEO-*b*-PS) diblock copolymer having a number-average molecular weight ($\overline{M}_n$) of 11 000 g/mol in the PEO blocks and an $\overline{M}_n$ of 5200 g/mol in the PS blocks has been synthesized (with a volume fraction of the PEO blocks of 0.66 in the molten state). Differential scanning calorimetry results show that this copolymer possesses a single endotherm, which is attributed to the melting of the PEO-block crystals. Based on real-time resolved synchrotron small-angle x-ray scattering (SAXS) observations, the diblock copolymer is in a disordered state above the glass transition temperature of the PS-rich phase (T_g^{PS}), which has been determined to be 44.0 °C during cooling using dilatometer mode in thermomechanical measurements. The order-disorder transition temperature (T_{ODT}) for this diblock copolymer is thus experimentally inaccessible. Depending upon different isothermal crystallization temperatures quenched from the disordered state (T_qs), four cases can be investigated in order to understand the phase relationships among self-organization, crystallization of the PEO blocks, and vitrification of the PS-rich phase: the region where the T_q is above the T_g^{PS}, the regions where the T_q is near but slightly higher or lower than the T_g^{PS}; and the region where the T_q is below the T_g^{PS}. Utilizing simultaneous SAXS and wide angle x-ray-diffraction experiments, it can be seen that lamellar crystals of the PEO blocks in the first case grow with little morphological constraint due to initial disordered phase morphology. As the T_q approaches but is still slightly higher than the T_g^{PS}, as in the second case, the PEO-block crystals with a greater long period (L) than that of the disordered state start to grow. The initial disordered phase morphology is gradually destroyed, at least to a major extent. When the T_q is near but slightly lower than the T_g^{PS}, the crystallization takes place largely within the existing phase morphology. Only a gradual shift of the L towards smaller q values can be found with increasing time, which implies that the initial phase morphology is disturbed by the crystallization of the PEO blocks. In the last case, the PEO blocks crystallize under a total constraint provided by the disordered phase morphology due to rapid vitrification of the PS-rich phase. Substantial decrease of crystallinity can be observed in this case. This study also provides experimental evidence that the PS-rich phase size, which is down to 7–8 nm, can still retain bulky glassy properties. [S0163-1829(99)01138-8]

I. INTRODUCTION

During the past 20 years, extensive research related to amorphous diblock copolymers has been carried out. In most cases, microphase separation is driven by the immiscibility between the block copolymer components, which are covalently linked. Theoretically, two limiting segregation regimes have been recognized, i.e., the strong segregation limit (SSL) and the weak segregation limit (WSL).[1] In the SSL regime, a variety of ordered morphologies, such as lamellas, gyroids, cylinders (hexagonal), and spheres (body-centered cubic), have been found as a consequence of minimizing free energy of the system by balancing interfacial energy, chain stretching, and maintaining constant density.[2] In the WSL regime, the order-order phase transition, the order-disorder transition (ODT), and the structures of disordered states are among the most attractive subjects. It was proposed that after the system enters the disordered state, two temperature regions may be recognized.[3,4] One at high temperatures can be described by the mean-field theory (MFT),[5] which assumes that the disordered phase is a homogeneous phase. The low-temperature region, which is close to the ODT temperature (T_{ODT}), can be best illustrated by the composition fluctuation theory (CFT).[6] In this region the disordered phase may retain some structural features caused by local concentration fluctuations. Recently, fluctuation-induced disordered structure has been studied experimentally by different groups.[7,8] They have proposed that the dynamic structure induced by the composition fluctuations in the disordered state close to the ODT very much resembles the late stage spinodal decomposition in homopolymer blends, i.e., a bicontinuous structure composed of block-*A*-rich and block-*B*-rich domains with a diffuse sinusoidal-wave-type profile interface.

For amorphous diblock copolymers, ordered phase mor-

 ©1999 The American Physical Society

phologies can be observed when the glass transition temperatures (T_gs) of the two phase-separated components are lower than the T_{ODT}. If T_g is higher than the T_{ODT}, on the other hand, only the disordered phase morphology is found. However, crystalline-amorphous diblock copolymers possess more complicated phase behavior due to the crystallization of the crystallizable component. One case occurs when the diblock copolymer components are miscible and form single phase in the melt, such as poly[ethylene-*b*-(ethylene-*alt*-propylene)] (PE-*b*-PEP),[9,10] and poly(ethylene oxide-*b*-methyl methacrylate) (PEO-*b*-PMMA).[11] When the T_g of the miscible copolymer is lower than the isothermal crystallization temperature of the crystallizable component quenched from the melt (T_q), the final microphase separation is actually driven by the crystallization of this component, and a lamellar morphology, in which the lamellar crystals are sandwiched by the amorphous-block layers, is always observed after crystallization. In an immiscible crystalline-amorphous diblock copolymer system, it can be expected that self-organization of the diblock copolymer, vitrification of the amorphous block, and crystallization of the crystallizable block may compete with one another in forming the final morphologies at different temperatures. Three temperature parameters need to be considered to describe the competitions: the T_{ODT}, the T_g of the amorphous phase, and the T_q [always lower than the melting temperature (T_m) of the crystalline blocks]. Generally speaking, the ODT is under thermodynamic equilibrium while crystallization requires undercooling, and vitrification is cooling-rate dependent.

Considering phase relationships in a case of $T_{ODT} > T_q > T_g$ (amorphous), examples can be found in the cases of poly(ethylene-*b*-ethylethylene) (PE-*b*-PEE),[12,13] poly(ε-caprolactone-*b*-butadiene) (PCL-*b*-PB),[14] poly(ethylene oxide-*b*-butylene oxide) (PEO-*b*-PBO),[15] poly(ethylene oxide-*b*-ethylethylene) (PEO-*b*-PEE), and poly[ethylene oxide-*b*-(ethylene-*alt*-propylene)] (PEO-*b*-PEP),[16] and others. Disregarding the initially ordered phase morphologies formed below T_{ODT}, crystallization of the crystallizable blocks usually occurs with little morphological constraint of the ordered phase, and finally, this process breaks apart the initial phase morphology to form crystalline lamellas. Therefore, the memory of the initial phase morphology is completely lost. Recently, it was also reported for some polyethylene containing diblock copolymers that when the crystallization rate of the crystallizable component with high molecular weight is fast (only local segmental rearrangement is expected during the crystallization), the phase morphology may be preserved at least to a certain extent.[17–19]

It has also been found that when the overall molecular weight of the diblock copolymers decreases, the T_{ODT} can be reduced. This leads to another case of $T_q > T_{ODT} > T_g$ (amorphous) in many systems, such as PE-*b*-PEE,[12] PCL-*b*-PB,[14] and PEO-*b*-PBO.[20] The lamellar crystal morphology is also found disregarding the initial phase morphology of the disordered state.

On the other hand, when a case of $T_{ODT} > T_g$ (amorphous) $> T_q$ is considered, the crystallization of the crystallizable blocks occurs within the ordered phase morphology. The crystallization is completely constrained due to the rapid vitrification of the amorphous blocks, as found in the cases of poly(tetrahydrofuran-*b*-methyl methacrylate) (PTHF-*b*-PMMA),[21] and poly(ethylene-*b*-vinyl cyclohexane) (PE-*b*-PVCH).[22] The initially ordered phase morphology is thus retained. Recently, a study of PCL-*b*-PS diblock copolymer was attempted in order to correlate the polystyrene blocks' vitrification effect with the PCL blocks' crystallization.[23] A PE-*b*-PS system with crystallizable PE block was also reported.[24] Another approach was done by crosslinking the PB component of a PCL-*b*-PB diblock copolymer.[25] The PB component becomes solidlike after crosslinking, and thus, crystallization of the PCL block can only more or less take place under the constrained phase morphology. As a result, the memory of the phase morphology is at least to some degree preserved.

In this study, a diblock copolymer of PEO-*b*-PS having $\bar{M}_n$s of 11 000 g/mol (11*k*) for the PEO blocks and 5200 g/mol (5.2*k*) for PS blocks, has been investigated. It is interesting to observe that this copolymer shows specific phase structural and morphological relationships based on the competitions among self-organization, vitrification, and crystallization in forming the final phase morphologies at various temperatures.

II. EXPERIMENTAL SECTION

Material and sample preparation

The diblock copolymer, PEO-*b*-PS with $\bar{M}_n$s of 11*k* for the PEO blocks and 5.2*k* for the PS blocks, was synthesized *via* anionic polymerization. The detailed procedure can be found in Ref. 26. In brief, the polymerization started with an anionic polymerization of styrene in benzene under a high vacuum at room temperature, using *sec*-butyl lithium as initiator.[27] The resulting poly(styryl)lithium was functionalized with ethylene oxide.[28] Dimethylsulfoxide (33 vol %) and a potassium salt (e.g., potassium *t*-amyloxide, 0.14 equiv.) were then added to the polymeric lithium alkoxide solution.[26] The ethylene oxide polymerization was carried out at 45 °C for 6 days. After termination with 0.1 M methanolic HCl, the crude polymer was purified by precipitation into hexanes for several times. The crude polymer contained a small amount of PEO homopolymer, because of the homopolymerization of ethylene oxide initiated by the potassium salt. The PEO homopolymer was removed by column chromatography on microcrystalline cellulose using methanol as eluent solvent. The PS precursor was characterized by size exclusion chromatography (SEC), and had an $\bar{M}_n$ of 5.2*k* and molecular weight distribution of 1.05. The $\bar{M}_n$ of PEO blocks was determined by ^{1}H NMR to be 11*k*, and the molecular weight distribution of the final diblock copolymer was determined by SEC to be 1.07. The volume fraction of PEC blocks was thus 0.66 in the melt. The density of amorphous PS is 1.052 g/cm^3, and the densities of amorphous and crystalline PEO are 1.124 and 1.239 g/cm^3, respectively.[29]

In order to ensure the consistency of the same phase behavior, uniform sample preparation procedure and thermal history were necessary. The sample was cast from a 5 w/v % toluene solution, and the solvent was allowed to evaporate over three days at room temperature. The residual solvent was further removed under vacuum at 50 °C, and then annealed at 70 °C for 24 h. The sample was then studied using different experiments of this study. It was found that phase

equilibrium could be reached after sample was treated via this annealing process. This thermal history was thus utilized for all of the diblock copolymer samples before the experiments were conducted.

Equipment and experiments

Time-resolved synchrotron small-angle x-ray-scattering (SAXS) and wide-angle x-ray-diffraction (WAXD) experiments were simultaneously conducted at the synchrotron x-ray beamline X27C of the National Synchrotron Light Sources in Brookhaven National Laboratories. The wavelength of the x-ray beam was 0.1307 nm. Isothermal crystallization measurements were carried out on a customized two-chamber hot stage. The T_q was controlled to be within ± 0.1 °C. The sample was preheated to 70 °C in a melting chamber, and held there for 3 min. It was then jumped to T_qs for isothermal crystallization. A heating rate of 1 °C/min was used to study the crystal-melting behavior of the sample after isothermal crystallization. One-dimensional position sensitive detectors (PSD's) were used to record the scattering and diffraction patterns. The zero pixel was calibrated using a duck tendon, and scattering vector q ($q = 4\pi \sin\theta/\lambda$, where λ is the wavelength of synchrotron radiation, and 2θ is the scattering angle) was determined with silver behenate. The Lorentz correction was performed by multiplying the relative intensity (I, counts per second) by q^2. The WAXD PSD was calibrated using Lupolen of a known crystal size. For long time isothermal crystallization experiments, conventional SAXS and WAXD were utilized, which were equipped with a 18 kW rotating anode and one-dimensional PSD's. The collimation was conducted using a combined slit and pinhole system designed in our laboratory. The calibration of the SAXS was the same as that in the synchrotron experiments. The final results were desmeared.

Differential scanning calorimetry (DSC, TA-2000 system) experiments were carried out to study the isothermal crystallization and melting behavior of the PEO-*b*-PS (11–5.2*k*). The DSC was calibrated with *p*-nitrotoluene, naphthalene, and indium standards. The sample weight was maintained at approximately 0.5 mg and the pan weights were kept constant to within ± 0.002 mg. Isothermal crystallization was conducted by quenching the sample from the disordered state at 70 °C to a preset T_q. The fully crystallized sample was then heated to above the T_m at a heating rate of 5 °C/min. The weight percentage crystallinity was calculated using an equilibrium heat of fusion for a perfect PEO crystal (8.66 kJ/mol).[30] The endothermic peak temperature observed during heating was taken as the T_m.

Dilatometry experiments were carried out in a thermomechanical (TM) analyzer (TA-TMA 2940). A bulk sample with a weight of about 20 mg was prepared in an aluminum cup having a diameter of 3 mm and thickness of 2 mm. The sample was freed of bubbles by annealing at 70 °C under vacuum for 24 h. A smooth and flat surface was necessary in order to obtain precise measurements of the linear thermal expansion using TM dilatometer mode. Different external stresses ranging from 0.127 to 0.318 MPa were applied to measure the sudden change of coefficients of thermal expansion (CTE) during cooling. Note that the heating experiments can also be performed in a similar way, but the results are obscured by the crystallization of the PEO blocks. The temperature where the sudden changes of the CTE occurred was defined as an apparent T_g under a particular external stress. The cooling rate was 2 °C/min. An extrapolation to the zero external stress was necessary for obtaining a precise T_g.

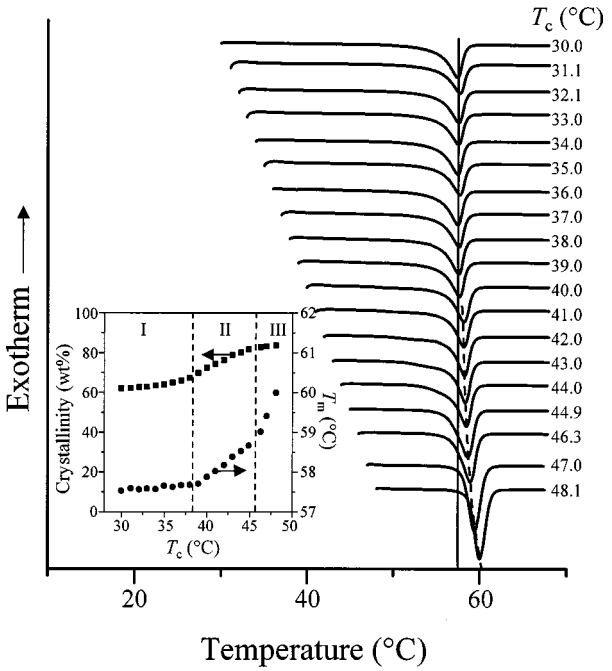

FIG. 1. DSC heating diagrams of the PEO-*b*-PS (11–5.2*k*) after crystallization at different temperatures. The heating rate was 5 °C/min. The inset shows melting temperature and crystallinity changes with isothermal T_q observed by DSC.

III. RESULTS AND DISCUSSION

General phase behavior of the diblock copolymer

DSC heating diagrams in Fig. 1 show a single melting endotherm for the diblock copolymer PEO-*b*-PS (11–5.2*k*) after complete crystallization at each T_q. This endothermic process is clearly attributed to the crystal melting of the PEO blocks. The T_m appears at a constant temperature of 57.5 °C when the T_q is below 38.0 °C. Between $T_q = 38.0$ and 46.0 °C, the T_m gradually increases with increasing T_q. After $T_q = 46.0$ °C, the increase of the T_m speeds up, and finally, it reaches 60 °C at $T_q = 48.1$ °C. It is also found that the DSC results are only dependent upon the T_q and the isothermal time (t_q), and independent of the resident time of the samples held at 70.0 °C when the time exceeds 3 min.

The inset of Fig. 1 provides the T_m and crystallinity dependence on isothermal T_qs. Three T_q regions can be identified based on the T_m changes as described in the previous paragraph (dashed vertical lines in the inset). It is interesting that three regions in the crystallinity changes of the PEO blocks can also be observed: a slight increase from 62% at $T_q = 30.0$ °C to 65% at $T_q = 38.0$ °C in region I; a gradual increase to 82% as T_q reaches 46.0 °C (region II); and a plateau of the crystallinity (82%) in region III with further increasing T_q.

The inset of Fig. 2 shows a set of SAXS results recorded during heating at 1 °C/min in the melt. It is evident that a scattering peak can be seen at $q = 0.367$ nm^{-1} at 50.0 °C (a ''long period'' $L = 2\pi/q = 17.1$ nm). With increasing temperature, this peak gradually shifts to higher q values, and its

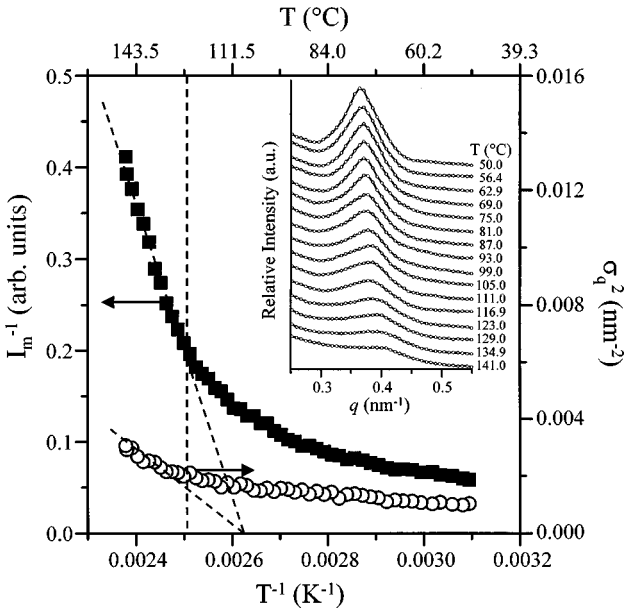

FIG. 2. Relationships between the reciprocal x-ray-scattering intensity and square of half width at half height (σ_q) with respect to reciprocal temperature. The inset is the SAXS results of the PEO-*b*-PS (11–5.2*k*) at different temperatures in the molten state.

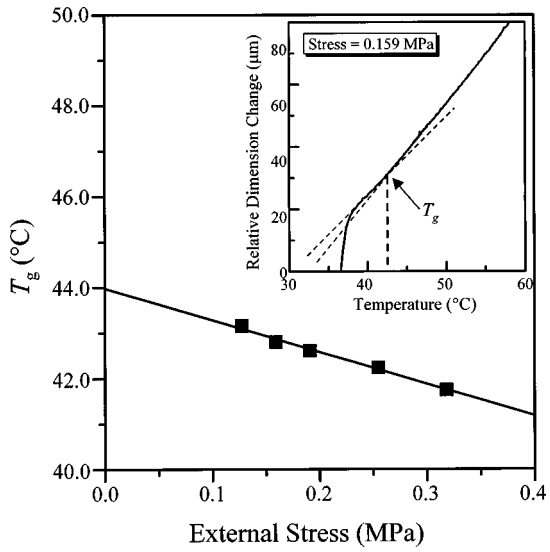

FIG. 3. Extrapolations of the T_g with different external stresses applied. The inset is a cooling curve of dialatometry data for the PEO-*b*-PS (11–5.2*k*) under an external stress of 0.159 MPa.

intensity decreases and the width at half maximum increases. No second-order scattering peak can be found in this figure. Based on this scattering profile, it can be qualitatively concluded that this sample is in a disordered state in the temperature range studied. This scattering peak is so-called the correlation hole scattering originated from the local density fluctuation of the two components in the diblock copolymer.

When the relationship between the reciprocal maximum intensity (I_m^{-1}) and reciprocal temperature (T^{-1}) is plotted, an initially linear decrease at higher temperatures can be seen followed by a nonlinear decay at lower temperatures,[3,4] as shown in Fig. 2. No sudden discontinuous change of the reciprocal intensity at a low temperature can be found at $T \geqslant 50.0\,°C$. In this figure, the square of the half width at half maximum (σ_q) data is also included, and a similar relationship with respect to T^{-1} can be observed (Fig. 2). Both observations indicate that the ODT of the sample is not found above 50.0 °C. As shown in Fig. 2, the linear relationship between the I_m^{-1} and T^{-1} at higher temperatures ($>125\,°C$) indicates that the disordered state can be described by the MFT,[5] while the nonlinear relationship at lower temperatures represents the disordered state which can be described by the CFT.[6] It is important to note that in the fluctuation-induced disordered phase, both the PEO-rich and PS-rich microdomains possess the sinusoidal-wave-type profile interface.[7,8]

The phase behavior of the PS-rich blocks needs attention. For block copolymers, such as PEO-*b*-PS with the PS block being the minor component and in the disordered state, the T_g of the PS-rich blocks is often difficult to observe in DSC. Methods such as dynamic mechanical, thermomechanical, dielectric, and solid-state nuclear magnetic resonance could be used to detect the T_g. The inset of Fig. 3 shows dilatometry results for the PEO-*b*-PS (11–5.2*k*) during cooling under an external stress of 0.159 MPa. It is evident that a sudden change of the CTE around 42.8 °C can be found upon cooling, representing a T_g. An abrupt decrease in dimension at 37 °C indicates the onset of crystallization of the PEO blocks. Under a stress of 0.318 MPa, the T_g occurs at 41.8 °C. It is thus slightly decreased with increasing the external force applied. Extrapolations to zero external stress yield an accurate T_g of 44.0 °C during cooling (Fig. 3), which represent the T_g of PS-rich phase (T_g^{PS}). Note that a pure PS with the same molecular weight (5.2*k*) possesses a T_g of 82 °C, while the amorphous PEO show a T_g of −67 °C.[30] Based on the relationship of diluent effect on a polymer's T_g,[31] it can be roughly estimated that in the PS-rich phase, the PEO component is about 15 wt %.

When we consider the three regions observed in T_m and crystallinity changes with T_q, it becomes evident that region I roughly corresponds to the system below the T_g^{PS}, region II is within the T_g^{PS}, and region III is above the T_g^{PS}. Therefore, these changes in T_m and crystallinity in the three regions may reflect the PEO-block crystallization under different environments (confined *versus* nonconfined).

The case of T_q above T_g^{PS}

When the diblock copolymer is crystallized above the T_g^{PS} at 48.0 °C, the evolution of the crystal structure, phase and crystal morphologies, and crystallinity can be followed by SAXS and WAXD experiments as shown in Figs. 4(a) and 4(b). It is evident that from SAXS data [Fig. 4(a)] the phase morphology formed in the disordered state can be observed in the initial stage of the experiment at the $L = 17.1$ nm, where the crystallization has not taken place. This is because crystallization needs a rather long induction time at this relatively low undercooling [Fig. 4(b)]. However, as soon as crystallization starts, a new L appears at $q = 0.245$ nm^{-1} ($L = 25.6$ nm, taken from the maximum intensity), while the scattering intensity of $L = 17.1$ nm representing the initial disordered phase morphology gradually decreases. This indicates that the phase morphology cannot be sustained during the crystallization of the PEO blocks. With increasing t_q, the intensity of the disordered scattering further decreases and

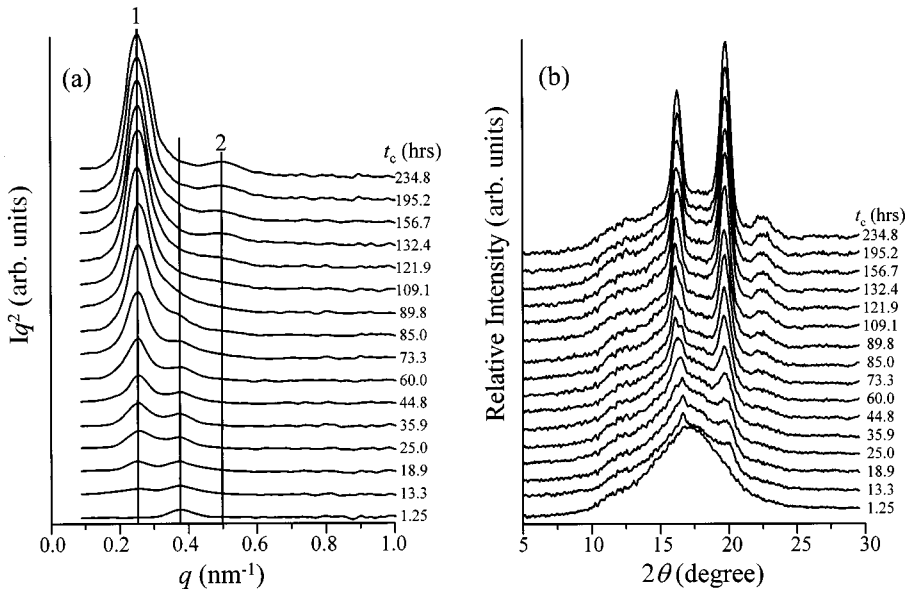

FIG. 4. Sets of SAXS (a) and WAXD (b) results of the PEO-*b*-PS (11–5.2*k*) crystallization at 48 °C at different isothermal times.

eventually vanishes after the complete crystallization of the PEO blocks. It is also important to find that in Fig. 4(a) the second-order scattering peak exists in the late stages of the crystallization, revealing a lamellar crystal morphology with alternating PEO lamellar crystals and PS-rich layers. This observation is consistent with many experimental findings reported previously that the initial phase morphology is always replaced by the lamellar crystal morphology when T_q is above the T_g associated with the amorphous blocks. In Fig. 4(b), the PEO-*b*-PS diblock copolymer gives the same WAXD patterns as PEO homopolymers, indicating that the PEO blocks crystallize in the same crystallographic structure as the pure PEO.

Figures 5(a)and 5(b) show SAXS and WAXD results of the diblock copolymer during heating after it is fully crystallized at 48.0 °C. With increasing temperature, the q value for the first-order scattering peak remains nearly constant in the SAXS pattern. This implies that above the T_g^{PS} the lamellar crystal morphology is stable up to its T_m at a heating rate of 1.0 °C/min. Therefore, the metastability of the crystal is not changed during heating at 1.0 °C/min. At 57.5 °C, the PEO crystals start to melt, evidenced by a decrease of the crystallinity as shown in the WAXD results [Fig. 5(b)]. This is also seen in the DSC heating diagram in Fig. 1. The scattering peak of the disordered state returns following the crystal melting.

The case of T_q slightly higher than the T_g^{PS}

When the crystallization of the sample is carried out at 45.0 °C, the T_q is slightly higher (1.0 °C) than T_g^{PS} but still within the glass transition region. Figures 6(a) and 6(b) show both SAXS and WAXD results recorded in this experiment. From the SAXS results, it is interesting that in the initial period of time of this experiment the scattering peak at $q = 0.376$ nm^{-1} ($L = 17.1$ nm) is attributed to the disordered phase morphology up to 17.5 min. With increasing t_q, the crystallization starts at 22.5 min, evidenced by the appearance of Bragg reflections in the WAXD experiment [Fig. 6(b)] and the increase of SAXS scattering peak intensity

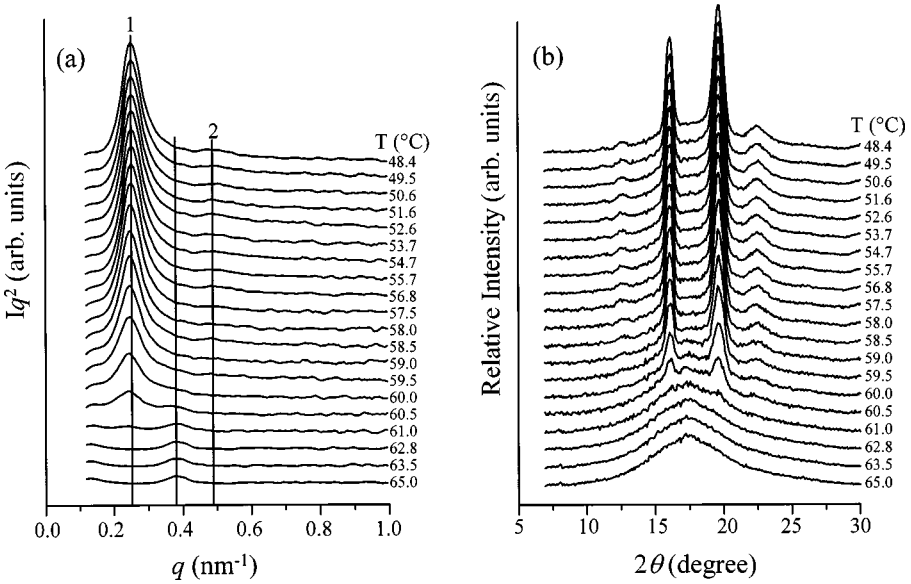

FIG. 5. Sets of SAXS (a) and WAXD (b) heating results of the PEO-*b*-PS (11–5.2*k*) after crystallization at 48 °C at a heating rate of 1 °C/min.

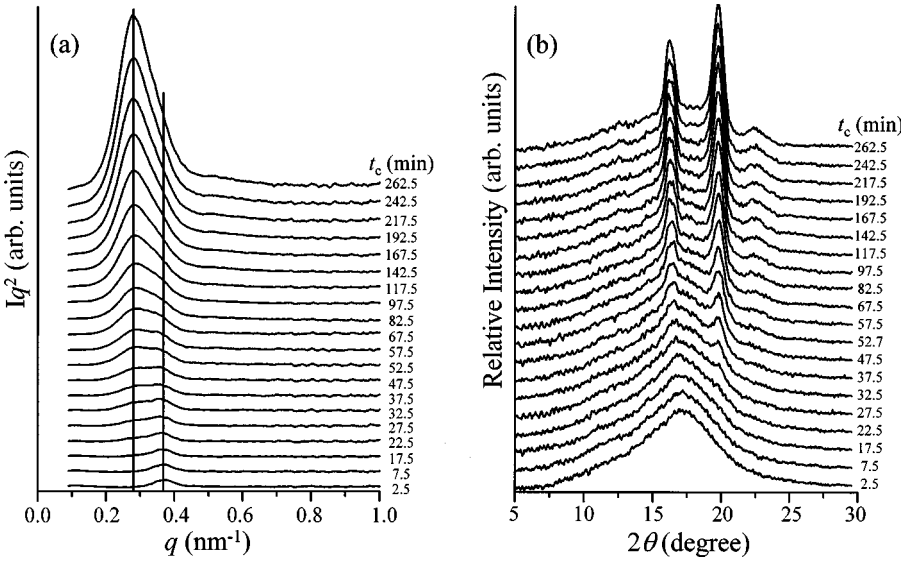

FIG. 6. Sets of SAXS (a) and WAXD (b) results of the PEO-*b*-PS (11–5.2*k*) crystallization at 45 °C at different isothermal times.

[Fig. 6(a)]. Another L, however, appears at a lower q value (0.270 nm^{-1}, $L=23.3$ nm), and its intensity increases significantly with t_q. No second-order scattering can be observed at $t_q<192.5$ min. A weak second-order scattering peak of the L can be seen after that t_q. It is also noted that the half width at half maximum for the crystal scattering is broader than that for the sample isothermally crystallized at 48.0 °C. On the other hand, the scattering peak at $q=0.376$ nm^{-1} gradually decreases in its intensity but it is not completely vanished even at 262.5 min [Fig. 6(a)].

These experimental results indicate that final crystallization in this case exhibits a newly formed crystalline morphology, which attempts to replace the existing phase morphology. Since the T_q is within the T_g^{PS} region, the PS-rich phase in the phase morphology tends to solidify. When the crystallization starts, this constraint may not be strong enough to confine the PEO blocks during the crystallization. This is because the temperature of 45.0 °C is slightly higher than the T_g^{PS} and complete solidification cannot be achieved. The crystallization may possess a stronger interaction to overcome the constrained geometry caused by the PS-rich phase and rearrange the PEO block to form the crystals with a greater L as shown in Fig. 6(a). During crystallization of the PEO blocks, the phase morphology is gradually and, at least partially, broken down. However, even for the new L at 23.3 nm, its second-order scattering peak is difficult to be observed [Fig. 6(a)], reflecting a residual effect of the initial phase morphology on this newly formed crystal morphology.

Figures 7(a) and 7(b) are the heating experiments recorded in both SAXS and WAXD after the sample was fully crystallized at 45.0 °C. The L increases after the temperature increases to 52.6 °C, indicating that the PEO-block crystals are able to effectively thicken during heating to about 10 °C higher than T_g^{PS} to perfect the crystals. On the other hand, crystal melting can be seen at around 55.0 °C [Fig. 7(b)]. This increase of the L at temperature higher than 55.0 °C may also result from a partial melting of the lamellar crystals. The crystallinity then drastically decreases with increasing temperature, indicating that a massive melting process takes place.

The case of T_q slightly lower than the T_g^{PS}

When the T_q is at 41.0 °C, which is slightly lower (3.0 °C) than the T_g^{PS}, the PEO blocks' crystallization behavior ex-

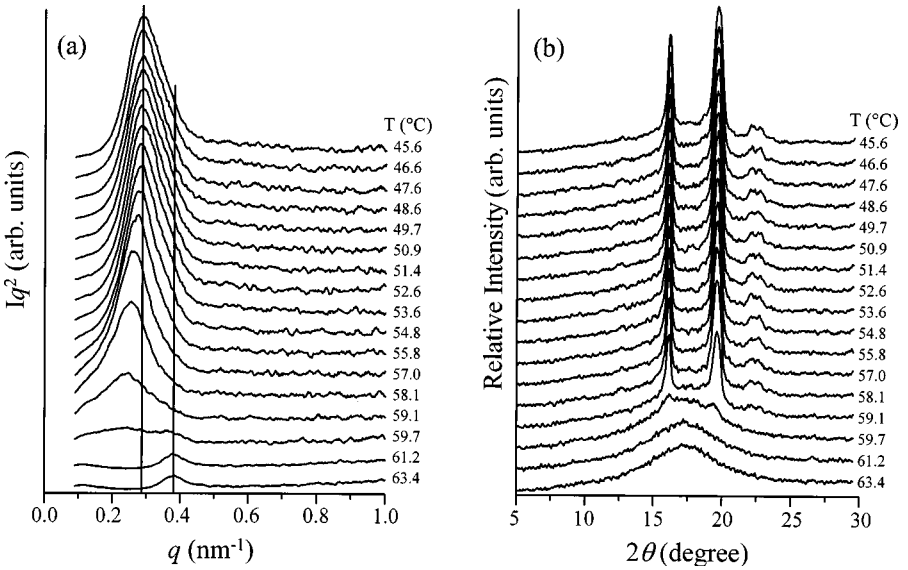

FIG. 7. Sets of SAXS (a) and WAXD (b) heating results of the PEO-*b*-PS (11–5.2*k*) after crystallization at 45 °C at a heating rate of 1 °C/min.

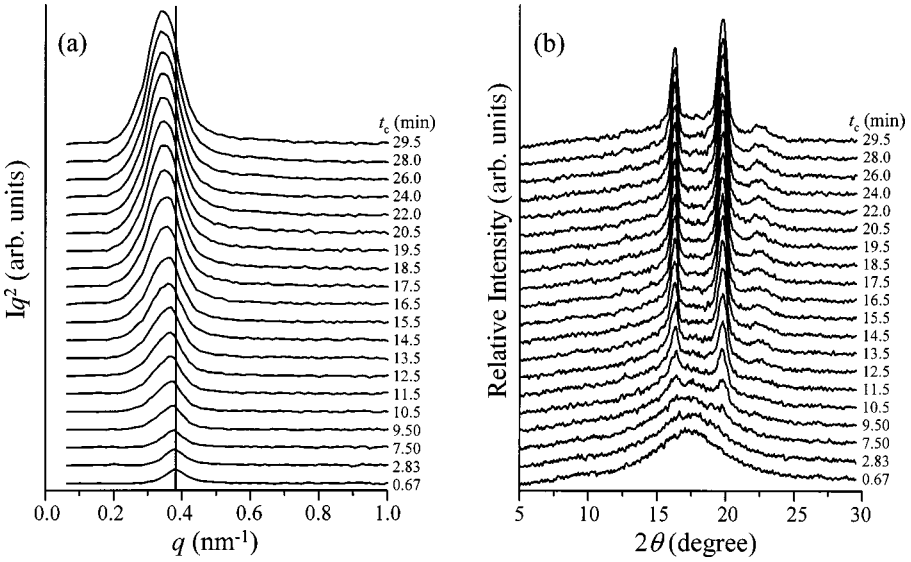

FIG. 8. Sets of SAXS (a) and WAXD (b) results of the PEO-*b*-PS (11–5.2*k*) crystallization at 41 °C at different isothermal times.

hibits substantial changes. Figures 8(a) and 8(b) show both SAXS and WAXD results of this experiment. From the SAXS data, it is interesting that in the initial period of t_q the scattering peak at $q=0.376$ nm^{-1} ($L=17.1$ nm) is attributed to the disordered phase morphology up to 2.8 min. With increasing t_q, the crystallization starts, evidenced by the appearance of Bragg reflections in the WAXD experiment [Fig. 8(b)] and the increase of peak intensity in the SAXS [Fig. 8(a)]. The L in this initial stage of crystallization, however, remains constant, which follows the L of the disordered phase morphology. As crystallization further proceeds, the enhanced scattering peak gradually shifts to lower q values and its intensity increases significantly with t_q. For example, at $t_q=12.5$ min, the L reaches 18.0 nm. Finally, at $t_q=29.5$ min, the L is 19.0 nm. This observation indicates that although the PEO blocks attempt to reach their most probable crystalline morphology, they are restricted by the PS-rich phase, which is very close to being a glassy solid.

These phenomena can also be found when the crystallization temperature is between 30 and 43 °C. However, shifts of the scattering peak become increasingly small when the T_q is reduced, indicating that the PS-rich phase becomes increasingly hardened towards the glassy solid, which in turn, generates more restrictions for the PEO blocks. For example, the final L stops at 17.3 nm at $T_q=30$ °C, 17.5 nm at $T_q=35$ °C, and 20.1 nm at $T_q=43$ °C. Generally speaking, the T_g of a polymer decreases when an external stress is applied to the polymer.[32] The crystallization of PEO blocks requires rearrangement of chain conformations and, therefore, space and chain mobility. This process may generate certain stresses on the PS-rich phase (at least at the interface), and therefore, the T_g^{PS} may be slightly reduced during crystallization. This is speculated to be the reason for the observed shift of the scattering peak, even 14 °C lower than the T_g^{PS} during the crystallization.

Figures 9(a) and 9(b) are the heating experiments recorded in both SAXS and WAXD after the sample was crystallized at 41.0 °C. The L starts to increase when temperature increases to 47.0 °C. This indicates that the PEO-block crystals can be annealed (thickened) after this temperature and the driving force of annealing and reorganization becomes dominant to change the metastability of the crystals.[33,34] On the other hand, the crystal melting starts at around 52.0 °C

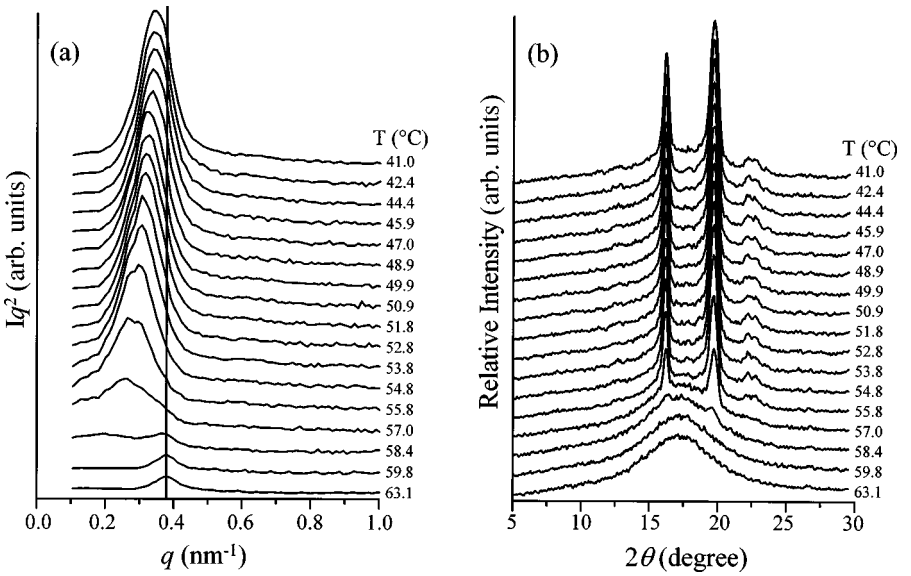

FIG. 9. Sets of SAXS (a) and WAXD (b) heating results of the PEO-*b*-PS (11–5.2*k*) after crystallization at 41 °C at a heating rate of 1 °C/min.

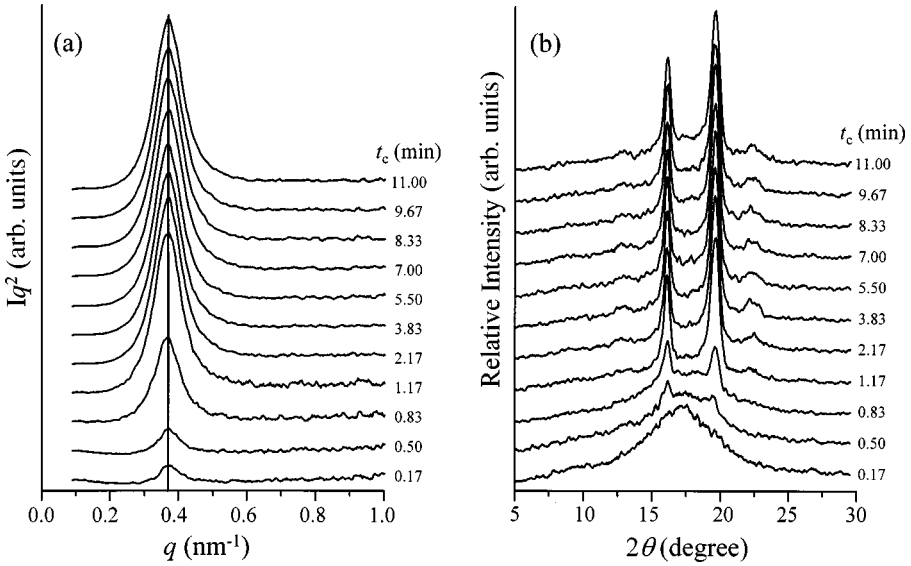

FIG. 10. Sets of SAXS (a) and WAXD (b) results of the PEO-*b*-PS (11–5.2*k*) crystallization at 27 °C at different isothermal times.

[Fig. 9(b)]. This increase of the L at temperatures higher than 52.0 °C may occur as a consequence of the partial melting of the lamellar crystal as well. The crystallinity drastically decreases with further increasing temperature (crystal melting).

The case of T_q below T_g^{PS}

As soon as the sample is quenched to well below the T_g^{PS}, the vitrification process occurs rapidly. In fact, a quick quenching may lead to a shift of the T_g^{PS} towards higher temperatures. Figure 10(a) shows a set of SAXS results during isothermal crystallization at 27.0 °C, which is 17.0 °C below the T_g^{PS}. Figure 10(b) is a set of corresponding real-time resolved WAXD data simultaneously recorded. For the first 0.17 min, SAXS results show a scattering peak at $L = 17.1$ nm. This peak possesses the identical intensity and the width at half maximum as those observed at high temperatures in the disordered state (Fig. 3), indicating that before crystallization of the PEO blocks, the system is still in the disordered state. No Bragg reflections in the WAXD experiments can be found during this short period of time. After $t_q = 0.5$ min, crystallization starts to occur, evidenced by substantial increases of the SAXS scattering [Fig. 10(a)] and Bragg reflection intensities [Fig. 10(b)]. A careful examination reveals that although the SAXS intensity significantly increases during the crystallization, the L of the scattering peak remains constant during the entire crystallization process. Note that no second-order scattering peak can be found even after complete crystallization. These results indicate that the crystallization of the PEO blocks can only proceed in this constrained phase morphology when the glassy phase is a continuous phase.

When heating the sample starting at 27.0 °C, the SAXS results show that in Fig. 11(a) the L does not change until 38.0 °C is reached. The L then thickens progressively up to 19.0 nm at 52.3 °C beyond which the crystal melting starts [Fig. 11(b)]. Note that this temperature of 38.0 °C where the thickening starts is 6.0 °C lower than the T_g^{PS} due to the driving force of crystal annealing which reduces the T_g. As long as the PEO-*b*-PS is crystallized below 30.0 °C, the onset of lamellar thickening is found to always be at 38.0 °C. These experimental results provide additional, though indirect, evidence that the PEO-block crystals can be annealed to break the geometrically constrained phase morphology only when

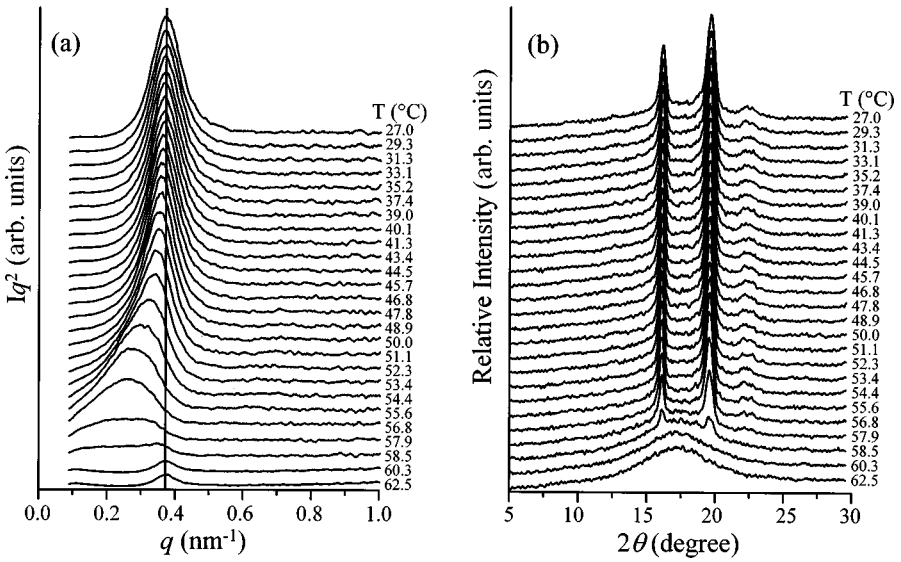

FIG. 11. Sets of SAXS (a) and WAXD (b) heating results of the PEO-*b*-PS (11–5.2*k*) after crystallization at 27 °C at a heating rate of 1 °C/min.

the T_q is in the vicinity or higher than the T_g^{PS}, depending on the metastability of the PEO-block crystals.

Finally, it is important to look into another perspective, which is also a direct consequence of this study: the lower limit of the glassy phase size. For many years, an interesting question has continuously come up, namely, how small can a phase be and still be called a phase? In other words, where is the lower limit of the phase size at which the macroscopic phase properties are still retained? Based on a simple calculation that converts the volume fraction of the copolymer components to the linear dimension (volume$\propto$length^3) under an assumption of a disordered two-phase model (the PEO phase and the PS-rich phase) as a first approximation, the size of the PS-rich phase should be close to 7–8 nm. We expect that a glassy state in polymers can exist at least down to this size range. The estimation of the size of PEO component is thus roughly 9–10 nm. Note that in a linear PEO with the same molecular weight, its L after being crystallized at 27 °C is estimated to be 15.0 nm,[35] which is much greater than the PEO-block crystal size in the diblock copolymer. This clearly demonstrates the constrained PEO-block crystallization caused by the PS-rich glassy phase. Furthermore, a 20% difference in the crystallinity of the PEO-block crystallized below and above the T_g^{PS} may provide another evidence for the constrained environment effect on crystallization.

IV. CONCLUSION

In a PEO-*b*-PS (11–5.2*k*) diblock copolymer crystallization of the PEO blocks can only take place from the disordered state, and the T_{ODT} is expected to be lower than the T_g^{PS} (44.0 °C). In order to study the phase relationships among self-organization, vitrification, and crystallization, four cases can be identified in this diblock copolymer based on the change of one temperature parameter T_q: the T_q is above the T_g^{PS}, the T_q is near but slightly higher or lower than the T_g^{PS}, and the T_q is below the T_g^{PS}. Based on our real-time synchrotron SAXS and WAXD experimental results, it is found that in the first case the PEO-block crystallization can take place with little phase morphological constraint since the PS-rich phase is in the liquid state (above the T_g^{PS}). In the second case, the constraints of the disordered state are relatively weak and the PEO blocks crystallize to form a greater L than that of the disordered state. After the crystallization process, however, the disordered phase morphology does not completely vanish, and the residual effect on the newly formed crystalline morphology still remains. In the third case, although the PS-rich phase has become close to the hard solid, the PEO-block crystallization can still manipulate the phase morphology by gradually shifting the L of the phase morphology towards lower q values. This manipulation substantially decreases with decreasing T_q and finally, this shift completely disappears when the T_q is below 30.0 °C, suggesting that the PEO-block crystallization become to be completely constrained by the vitrification of the PS-rich phase. This leads to the fourth case. It seems that in this diblock copolymer the size of the bulk glassy state can be estimated at least down to a vicinity of 7–8 nm.

ACKNOWLEDGMENTS

This research was supported by the National Science Foundation (DMR-9617030). Research was carried out in part at the National Synchrotron Light Source in Brookhaven National Laboratories, which is supported by the U.S. Department of Energy, Division of Material Science and Division of Chemical Sciences.

*Electronic address: cheng@polymer.uakron.edu

[1] F. S. Bates and G. H. Fredrickson, Annu. Rev. Phys. Chem. **41**, 525 (1990).
[2] E. Helfand, Macromolecules **8**, 552 (1975); see, also, E. Helfand and Z. R. Wasserman, *ibid.* **9**, 879 (1976).
[3] N. Sakamoto and T. Hashimoto, Macromolecules **28**, 6825 (1995).
[4] J. H. Rosedale, F. S. Bates, K. Almdal, K. Mortensen, and G. D. Wignall, Macromolecules **28**, 1429 (1995).
[5] L. Leibler, Macromolecules **12**, 1602 (1980).
[6] G. H. Fredrickson and E. Helfand, J. Chem. Phys. **87**, 697 (1987).
[7] F. S. Bates, J. H. Rosedale, and G. H. Fredrickson, J. Chem. Phys. **92**, 6255 (1990).
[8] N. Sakamoto and T. Hashimoto, Macromolecules **31**, 3815 (1998).
[9] P. Rangarajan, R. A. Register, and L. J. Fetters, Macromolecules **26**, 4640 (1993).
[10] P. Rangarajan, R. A. Register, D. H. Adamson, L. J. Fetters, W. Bras, S. Naylor, and A. J. Ryan, Macromolecules **28**, 1422 (1995).
[11] P. H. Richardson, R. W. Richards, D. J. Blundell, W. A. MacDonald, and P. Mills, Polymer **36**, 3059 (1995).
[12] A. J. Ryan, I. W. Hamley, W. Bras, and F. S. Bates, Macromolecules **28**, 3860 (1995).
[13] P. Rangarajan, R. A. Register, L. J. Fetters, W. Bras, S. Naylor, and A. J. Ryan, Macromolecules **28**, 4932 (1995).
[14] S. Nojima, K. Kato, S. Yamamoto, and T. Ashida, Macromolecules **25**, 2237 (1992).
[15] A. J. Ryan, J. P. A. Fairclough, I. W. Hamley, S.-M. Mai, and C. Booth, Macromolecules **30**, 1723 (1997).
[16] M. A. Hillmyer and F. S. Bates, Macromol. Symp. **117**, 121 (1997).
[17] A. K. Khandpur, C. W. Macosko, and F. S. Bates, J. Polym. Sci., Part B: Polym. Phys. **33**, 247 (1995).
[18] D. J. Quiram, R. A. Register, and G. R. Marchand, Macromolecules **30**, 4551 (1997).
[19] D. J. Quiram, R. A. Register, G. R. Marchand, and D. H. Adamson, Macromolecules **31**, 4891 (1998).
[20] Y. W. Yang, S. Tanodekaew, S.-M. Mai, C. Booth, A. J. Ryan, W. Bras, and K. Viras, Macromolecules **28**, 6029 (1995).
[21] L.-Z. Liu, F. Yeh, and B. Chu, Macromolecules **29**, 5336 (1996).
[22] I. W. Hamley, J. P. A. Fairclough, A. J. Ryan, F. S. Bates, and E. T. Andrews, Polymer **37**, 4425 (1996).
[23] S. Nojima, H. Tanaka, A. Rohadi, and S. Sasaki, Polymer **39**, 1727 (1998).
[24] F. S. Bates (private communication).
[25] S. Nojima, K. Hashizume, A. Rohadi, and S. Sasaki, Polymer **38**, 2711 (1997).
[26] R. P. Quirk, J. Kim, C. Kausch, and M. S. Chun, Polym. Int. **39**, 3 (1996).

[27] M. Morton and L. J. Fetters, Rubber Chem. Technol. **48**, 359 (1975).
[28] R. P. Quirk and J. Ma, J. Polym. Sci., Part A: Polym. Chem. **24**, 2031 (1988).
[29] B. Wunderlich, *Macromolecular Physics, Crystal Structure, Morphology, and Defects*(Academic, New York, 1973), Vol. 1.
[30] B. Wunderlich, *Thermal Analysis* (Academic, San Diego, 1990).
[31] T. G. Fox, Bull. Am. Phys. Soc. **1**, 123 (1956).
[32] F. A. Arnold, Jr., D. Shen, C. J. Lee, F. W. Harris, S. Z. D. Cheng, and H. W. Starkweather, Jr., J. Mater. Chem. **3**, 183 (1993).
[33] S. Z. D. Cheng and A. Keller, Annu. Rev. Mater. Sci. **28**, 533 (1998).
[34] A. Keller and S. Z. D. Cheng, Polymer **39**, 4461 (1998).
[35] S. Z. D. Cheng, J. S. Barley, A. Zhang, A. Habenschuss, and P. R. Zschack, Macromolecules **25**, 1453 (1992).